The cosmic ray spectrum at energies above 10^{17} eV

1973 J. Phys. A: Math. Nucl. Gen. 6 1612

(http://iopscience.iop.org/0301-0015/6/10/019)

J. Phys. A: Math., Nucl. Gen., Vol. 6, October 1973. Printed in Great Britain.

The cosmic ray spectrum at energies above 10^{17} eV

D M Edge, A C Evans†, H J Garmston, R J O Reid, A A Watson, J G Wilson and A M Wray

Department of Physics, University of Leeds, Leeds LS2 9JT, UK

Received 2 April 1973

Abstract. A determination of the total energy spectrum of primary cosmic ray particles for the energy range from 3×10^{17} eV up to about 10^{20} eV is reported. This is based on a ground parameter, given by measurements in deep water-Čerenkov detectors, chosen to have minimum sensitivity both to the nature of the primary particles (charge spectrum) and to details of nuclear interactions involved in shower development (introduced into the treatment as a series of models covering what are thought to be important possible features of interactions at extreme energies). It is accordingly largely free from uncertainties about both the charge spectrum and details of shower development.

The primary total energy integral spectrum:

$$I(>E_p) = (4{\cdot}5 \pm 0{\cdot}5)10^{-10}\left(\frac{E_p}{10^{17}}\right)^{-2{\cdot}17 \pm 0{\cdot}03} \quad \mathrm{m^{-2}\,s^{-1}\,sr^{-1}} \qquad (E_p \text{ in eV}),$$

is shown to hold between 3×10^{17} eV and 10^{19} eV, and the evidence is consistent with a continuation of this form up to about 10^{20} eV.

1. Introduction

The demonstration that cosmic ray primaries can carry energies of at least several times 10^{19} eV, and probably of 10^{20} eV and greater, is of direct cosmological importance, and this has in recent years been intensified by the conclusion of Greisen (1966), Zatsepin and Kuzmin (1966) and Hillas (1968) that the flux of microwave photons, if universal, should lead to an abrupt steepening of the spectrum of extragalactic particles, whether protons or heavier nuclei, somewhere in the range 10^{18}–10^{20} eV. Those experimental groups who have most recently published relevant data (Andrews *et al* 1971, Bell *et al* 1971, Kawaguchi *et al* 1971) agree in finding no indication of any such steepening of the spectrum. However, the critical standing of all these measurements cannot be claimed to have been fully examined, and while the total statistical evidence of what has been reported, if no other uncertainties remained in the observations, would probably be sufficient to establish the absence of any steepening significantly below 10^{20} eV, these measurements have to be seen against a history of major uncertainties and inconsistencies about the spectrum at such energies. The same reservations apply to the feature of these measurements which, in contrast with those reported during the previous decade, are best consistent with little or no change in the spectral index over the 10^{18}–10^{20} eV range rather than with the presence of a significant and fairly abrupt reduction in the slope of the spectrum which had been a feature of rather earlier work.

† Now at Ferranti Ltd, Bracknell, UK.

This paper presents a detailed analysis of data from the Haverah Park 2 km array over the period July 1968–December 1971, of the evaluation of this material and of conclusions derived from it relating to the spectrum. It is at a stage when the continuation of measurements is adding only slowly to the statistical significance of the data presented as these relate to the selected ground parameter, but when more rapid development of our understanding of the actual incident primary spectrum may be anticipated from aspects of work which improve the precision of individual measurements, and particularly from observations of shower features which will restrict the range of nuclear cascade models which are tenable, and which form the essential link between what is observed and the energy of primary particles.

2. Experimental material

The differential energy spectrum of primaries is derived from a set of measurements of intensity in a series of 'bins', each covering a limited range of the experimentally determined parameter, through some relationship which links this parameter with the primary spectrum. It is logical and important to maintain the distinction between conclusions about the measurement of such parameters and deductions from them about the primary spectrum, since the linking process is not yet well understood, and various forms of shower development theory should be capable of application to established ground data without ambiguity. In this section we are concerned specifically with ground data.

To measure the intensity over a selected range of the ground parameter, two distinct pieces of information are involved, the assignation of a value of the parameter to each recorded shower and, further, the determination as to whether or not each falls within a defined collecting area. It is not immediately evident that the procedures of selection for these two indispensible elements are not to some extent in conflict.

2.1. Selection of shower data

As in work previously reported from Haverah Park, the array (figure 1) was triggered whenever the energy loss in A1 and in two of A2, A3 and A4 exceeded 2·5 GeV (roughly corresponding to a density of 0·3 equivalent relativistic muons per square metre). The detector groups to which these figures refer have been described elsewhere (Tennent 1967). Each is made up of a number of water-Čerenkov detectors of area 2·3 m^2 and depth 1·2 m: they essentially measure the energy dissipation by shower particles in the water of the detectors, the contribution from individual muons being normally that associated with the traversal of the full depth of the detector by a relativistic muon, while that associated with the electromagnetic component corresponds to almost complete absorption. Showers recorded from July 1968–December 1971 were selected for the present analysis using three additional criteria:

(i) that all three triggering signals were greater than 3·75 GeV;
(ii) that all the detectors A1, A2, A3, A4 yielded measured signals;
(iii) that the shower axis fell within 60° of the zenith.

Criterion (i) was imposed since showers involving triggering signals close to threshold frequency yield data leading to poor core location, because of the inherent fluctuations in the smallest of these signals and of measurement errors in determining it. Criterion (ii) ensures that the accuracy of zenith angle determination is substantially constant for all

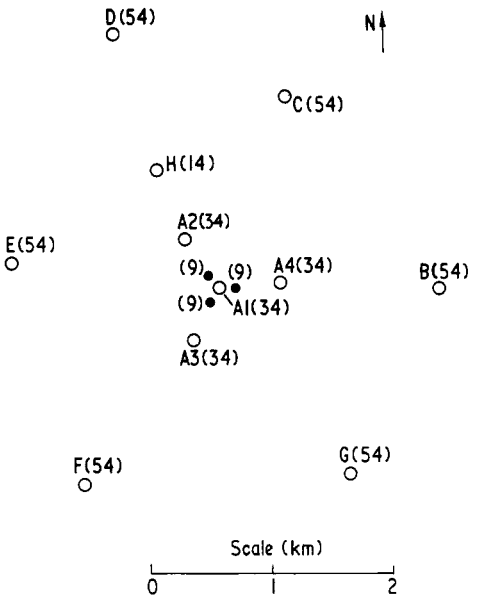

Figure 1. The Haverah Park detector array. The figures in parentheses show the area of each detector group in square metres.

selected data, while criterion (iii) sets the limit beyond which geomagnetic distortion becomes great enough to make a circularly symmetric analysis inadequate.

The total useful run-time was 27280 hours during the period in question, a recording efficiency of 89 % of all time, and a total of 3497 showers were selected for analysis.

2.2. Procedure for shower analysis

Density information from the 14 detector groups shown in figure 1 were used for the analysis of the selected shower. Although the detector-group configurations at B, C, D, E, F and G are in fact sub-arrays of geometry similar to, but smaller in scale than, that at A, for the present work each of the six outer groups was normally treated as a single (large) detector, and 'detector' in what follows includes each of these groups as one unit†. For showers from primaries of about 5×10^{17} eV, on average seven detector groups recorded nonzero signals, while at 5×10^{18} eV and 5×10^{19} eV the corresponding numbers were nine and eleven respectively.

Starting with an initial core (x_1, y_1) in a plane normal to the shower direction a gradient search method was used to minimize the function

$$\chi^2(x', y') = \sum_i (\sigma_i')^{-2}(\rho_i(r)-\rho_i'(r))^2, \tag{2.1}$$

where $\rho_i(r)$ is the observed density (energy absorption signal per unit area of the ith detector) at the perpendicular distance r from the trial core, x', y', where $\rho_i'(r)$ is the

† There are a few instances in which the individual detector groups of the outer sub-arrays (B, C, D, E, F, G) are usefully introduced separately: this is so when the core of a large shower falls rather near to that particular sub-array.

predicted density at that point for a trial shower size, and σ_i' is the expected uncertainty in $\rho_i'(r)$. The predicted density $\rho_i'(r)$ is calculated assuming:

$$\rho_i'(r) = kf(r), \tag{2.2}$$

where k is a constant determined by the shower size parameter (see § 2.3) and $f(r)$ is an empirically determined lateral distribution function of density (see § 2.4). The trial shower size is chosen by minimizing equation (2.1) at (x', y').

The choice of the initial trial core (x_1, y_1) for computer analysis presents considerable difficulties, if human intervention is to be kept as low as possible, since no prescription for its choice seems generally suitable for all possible shower core positions. In the event, a method based on the intersecting loci technique of Williams (1948) was used for the majority of analyses. The result of each analysis was scrutinized by an experienced observer, and for a bad analysis (usually, that is to say, one yielding a large value of χ^2, equation (2.1)) an alternative starting point was offered for a re-analysis. This scrutiny was of additional value since it revealed a number of data-handling errors.

It is worth noticing that the 'centre of gravity' method is unsatisfactory for finding a starting core, particularly when the true core is close to the array boundary. For then the χ^2 surface has multi-minima, some of which may be outside the boundary: the true core minimum may then be difficult to find unless special search techniques are used.

2.3. The shower size parameter

The shower size parameter used in the important early shower experiments (for example Clark *et al* 1961, Linsley 1963a) was the total number of shower particles N_e at the level of observation: since this number in fact differs very little from the total number of electrons, it is usually referred to as the 'number of electrons' to distinguish it, for example, from the much smaller number of muons. This parameter is directly applicable to data derived from detectors with yes/no characteristics, indicating whether or not one (or more) ionizing particle has traversed the detector: the thin-walled Geiger tube is such a detector, and use of this parameter developed from statistical treatments of the response pattern from multi-counter arrays. It is also closely applicable to signals derived from *thin* continuous detecting layers (eg thin scintillator sheets), but becomes less appropriate when the absorption thickness of the detecting layer is comparable to or greater than the range of the most absorbable shower particles (electrons) and tends to approach the interaction mean-free-path of the nonionizing (photon) component of the shower. Subject to these limitations, this parameter could be measured with good accuracy for small arrays with many detectors with which it was possible to measure the lateral distribution function to within small distances of the shower axis. However, with large arrays, using widely spaced detectors, it is difficult to have measurements closer than several hundred metres from the shower axis. The wide spacing of detectors is dictated by the very low rate of showers from high energy primaries: for example, the number of cores from a primary of even 10^{18} eV (still in the lower part of the range of the present work) falling within 100 m of a particular detector is only a few per year. At first sight this feature represents a serious defect of all arrays currently in operation to investigate features of the primary radiation above about 10^{17} eV.

A quite different complexion on the whole problem of shower studies at high energies comes, however, from a consideration of fluctuations in shower development. The importance of intrinsic fluctuations of shower development was realized at an early stage by the MIT group, who showed that these were of particular importance for

proton primaries, at depths of observation away from shower maximum, and near to the shower axis. Attempts were made to correct the primary energy spectrum derived from the sea-level number spectrum by allowing for fluctuations in the point of first interaction of the primary (Kraushaar 1958, Clark *et al* 1961), while later Linsley (1963b) showed that fluctuations of the location of later interactions were also important.

The availability of large numbers of computer-derived Monte Carlo simulations has in recent years enabled the fluctuation problem to be considered in more detail. These simulations have confirmed that fluctuations, if there are any, are particularly severe near the axis and for all types of detector responding strongly to the electromagnetic component of a shower. Accordingly, well chosen parameters now make no use for estimations of shower size of signals near to the shower axis†, and it has become important that where observational material is quoted in the form of values N_e, the convention used to represent the large but unmeasured number of particles falling within this central region should be clearly given.

Hillas and his co-workers (Hillas 1970, Hillas *et al* 1971a, b) investigated the fluctuation problem with particular reference to the Haverah Park array, and to the parameter $\rho(r)$ introduced in § 2.2. The figures of table 1 (reproduced in part from Hillas *et al* 1971a) show the RMS variation for a particular (generally plausible) shower model, expressed as a percentage, for a vertical proton primary of energy 10^{17} eV. The figures, given for various values of $\rho(r)$ and also for the total quantities N_e and N_μ (total number of muons) are intrinsic; they take no account of further limitations arising from actual procedures of observation. The small fluctuations of $\rho(476)$ and $\rho(951)$ arise because they correspond to values of r at which the average shower of this energy is near maximum development: for greater distances it has not yet reached maximum, for smaller distances it is already beyond it.

Table 1. Shower fluctuations of certain parameters: $E_p \sim 10^{17}$ eV

	$\rho(42)$	$\rho(119)$	$\rho(476)$	$\rho(951)$	$\rho_\mu(42)$	N_μ	N_e
RMS variation (%)	55	41	14	6	27	12	67

$\rho(r)$ is the deep water-Čerenkov response at distances in metres, $\rho_\mu(r)$ is the corresponding muon density.

The necessity, because of primary flux consideration, of making use of data derived far from the shower axis, is seen in table 1 to impose little impediment upon the choice of a good shower size parameter.

The use of Monte Carlo simulations allows other aspects of the effect of different shower size parameters to be quantified. The investigation can cover aspects as diverse as model changes, both for protons and for heavier nuclei, on the one hand and the actual sampling problem by detectors of limited area on the other. The sampling operation includes both the actual receptivity of the detector groups (for the large groups at A, 34 m^2 each) and the effects of this on shower analysis as these are further modified by the geometry of the array of detector groups which comprise the whole detecting system.

† The very reasons which make these near-axial signals unsuitable for use in the present context make them of particular interest in investigations of the nature of primary particles.

The Hillas simulations have been carried out for a variety of models (which will, of course, lead to changes in the figures of which an example is given in table 1). Overall, these show that when all features noted in the previous paragraph are combined, for showers of $E_p \sim 5 \times 10^{17}$ eV, the distance at which the Čerenkov signal is best determined is about 500 m, while at 5×10^{18} eV the corresponding distance is about 700 m. Throughout this paper, accordingly, the parameter chosen is $\rho(600)$; it is thus a compromise, but satisfactory insofar as the most favourable distance of measurement at a particular energy is not sharply defined. This parameter, with the provision currently available for measuring it, appears in its insensitivity to shower fluctuations and to measurement limitations to be superior to the other possibilities indicated in table 1.

However, for the immediate purpose of the present work, the determination of the total energy spectrum of incident primary particles, this parameter has a further advantage of crucial importance: the relationship between $\rho(600)$ and E_p is much less sensitive to model uncertainties than other parameters or than other values of $\rho(r)$. This is particularly so as it relates to the relationship of the slope of the $\rho(600)$ spectrum to that of the E_p spectrum. In this way it approaches as closely as any known to the important criterion indicated at the beginning of § 2. The way in which this property emerges in our actual conclusions about the E_p spectrum will appear in a later section. The reasons for this feature are complex, but at least one reason can readily be visualized. Shower models differ in the proportion of energy which they predict will go with the muonic and electromagnetic components. The parameter used here takes comparable amounts of signal from these two components, and so, to the first order, model variations altering this proportion do not change the measured quantity.

The parameter $\rho(600)$ is most accurately considered as measuring the energy loss by the shower complex in the detectors of the system, and an appropriate unit would be GeV m^{-2}. However, the detectors are calibrated with reference to the average signal produced by a single vertical relativistic muon, and in earlier work $\rho(r)$ has been stated in terms of this unit, that is, in terms of so many equivalent muons. To avoid confusion, this convention is continued in what follows.

2.4. Determination of the lateral distribution function

It would be possible to analyse the selected showers using either an empirically derived lateral distribution function or one predicted by model calculations. There are strong reasons for preferring the former procedure: the nature of the primary particle for each of these showers is not known, nor has the most correct model been identified. For these reasons an empirical function has been determined and used.

The selected showers were divided into eight bands of zenith angle: 0°–20°, 20°–30°, and then in 5° bands from 30° to 60°, and the lateral distribution function determined for each band in the following way.

A sub-selection of showers was made in which the core position and $\rho(600)$ could be well determined using three or four of the available density measurements. Such showers are typically those in which several density measurements are nearly equal, and are derived at points which encircle the core. These showers were analysed using only these densities, then the remaining measured densities were normalized by division by $\rho(600)$ and the lateral distribution function determined from a re-analysis of the complete set of showers: it was found to be rapidly convergent.

This method of using part of the data from certain showers to analyse them (ie to determine the size parameter $\rho(600)$) and the remaining data of these showers, together

with that from other showers, to determine the mean lateral distribution function of the whole group of showers is described as the 'redundant density' method: implicit in this method are the assumptions that the whole group can properly be analysed using a single function both from shower to shower of a particular size and over the whole range of shower sizes. The possibility of some variation is discussed in § 4.2 below.

In the present work we have used a function of the form $f(r) = r^{-\{\eta+(r/r_0)\}}$. With suitable empirical values of the parameters η and r_0, this function fits the experimental data well in the distance range 50 m $< r <$ 1500 m. It has been used in preference to the form $f(r) = (1/r)\{1+(r/r'_0)\}^{-(\eta'-1)}$ used in earlier work (Andrew *et al* 1971) because it can be fitted to the experimental data over a wider range of distances. For $r \ll r'_0$ the earlier function reduces to $1/r$, which is flatter than the experimental results indicate, but over the distance range 100 m $< r <$ 1000 m, which is the most important for the determination of the size parameter $\rho(600)$, the two functions are not very different. For example, for a vertical shower of size $\rho(600) = 1{\cdot}0\ \mathrm{m}^{-2}$, the signals shown in table 2 were obtained for various other distances using values of η and r_0 respectively: $r_0 = 4000$ m, $\eta = 2{\cdot}3$; $r'_0 = 243$ m, $\eta' = 4{\cdot}51$.

The average values of the parameters η and r_0 directly obtained from the mode of analysis indicated for the eight zenith angle bands are shown in figure 2. Since we may

Table 2. Comparison of the adopted distribution function with that used by Andrews *et al* (1971)

	$\rho(50)$	$\rho(100)$	$\rho(300)$	$\rho(1000)$	$\rho(1500)$
$f(r) = r^{-\{\eta+(r/r_0)\}}$	754	143	8·4	0·14	0·02
$f(r) = \frac{1}{r}\left(1+\frac{r}{r'_0}\right)^{-(\eta'-1)}$	479	141	9·4	0·15	0·03

($\rho(r)$ in 'equivalent muons' m^{-2}.)

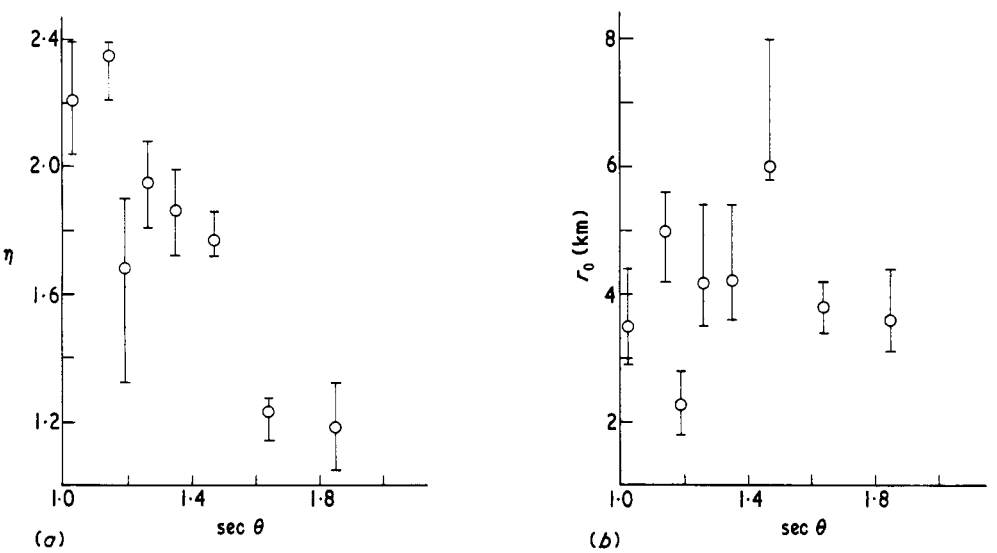

Figure 2. Data from eight zenith angle bands leading to the determination of the lateral distribution function for $0° < \theta < 60°$. (*a*) yields the variation of η with θ; (*b*) leads to the average value of r_0.

be confident that the values of these parameters over a series of arbitrarily defined bands must vary smoothly, we have treated r_0 as independent of zenith angle within the uncertainties of measurement, with the value $r_0 = 4000$ m, and, using this value, we have determined the best-fit values of η. These are well represented by:

$$\eta = 3{\cdot}78 - 1{\cdot}44 \sec\theta, \tag{2.3}$$

and the values of r_0 and η now given have been used in what follows. Figures 3 and 4 give examples of the application of this structure function to a wide range of sizes of near-vertical showers (figure 3) and of the difference of structure function for a near-vertical shower as compared with those in the limiting region of zenith angle approaching 60° (figure 4).

The variation of lateral distribution function with zenith angle has been compared with that predicted by Hillas using his preferred (proton primary) model, 'model E' (Hillas *et al* 1971b). For all zenith angles the agreement is good for 200 m $< r <$ 800 m, but at all zenith angles at small distances the observed distributions tend to be flatter, and at large distances steeper, than the theoretical distributions.

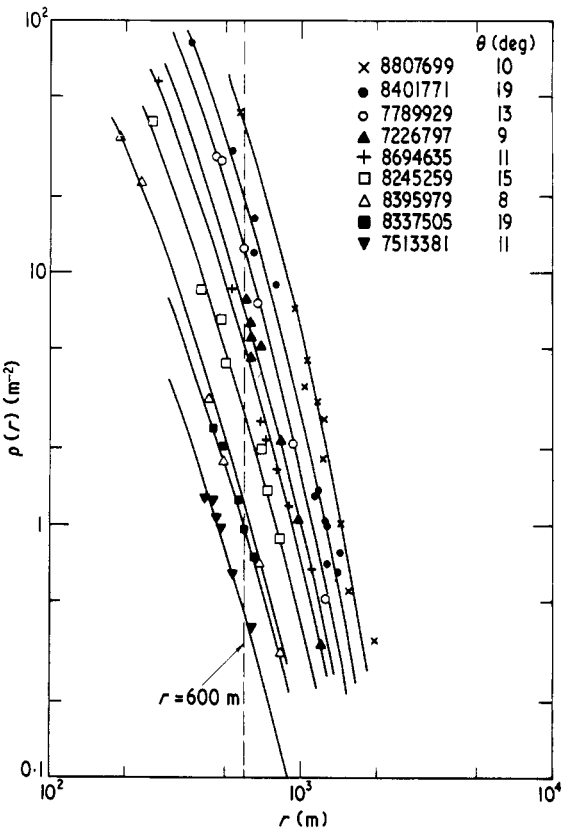

Figure 3. The vertical lateral distribution function for $\rho(r)$ fitted to a range of showers with $\theta < 20°$. The extreme showers shown are of approximate energies 3×10^{17} eV (7513381) and $2{\cdot}7 \times 10^{19}$ eV (8807699). A broken line at $r = 600$ m illustrates the relationship of $\rho(600)$ with the series of measurements for each shower.

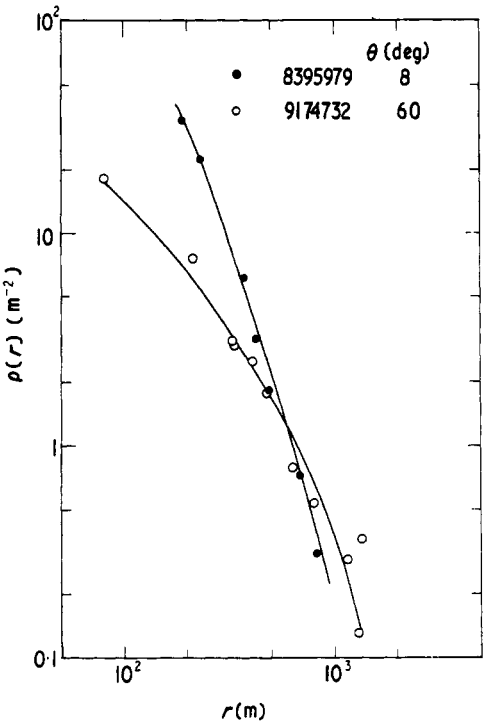

Figure 4. Variation of the lateral distribution function $\rho(r)$ between extreme values of the zenith angle θ.

2.5. Assessment of measurement errors

The likely errors of measurement in $\rho(600)$ have been estimated using simulated showers of nominal primary energy 10^{17} eV, 10^{18} eV and 10^{19} eV. Poissonian fluctuations and measurement uncertainties were included when determining the 'observed' density produced by each simulated shower at the detectors involved, and the shower was then analysed using the 'real' shower analysis program, due allowance being made for the possibility that, in any given shower, nontriggering detectors may have been inoperative. Showers were analysed with lateral distribution functions which were steeper, flatter or of the same form as that used to generate the observed densities. Only vertical showers were studied. Details of the methods used, and of the results, have been given by Evans (1971) and points relevant for the present work have been extracted in table 3.

Table 3.

Shower energy (eV)	Mean core displacement (m)	RMS variation of $\rho(600)$ (%)	Size change (%) when analysed with incorrect lateral distribution	
			10% 'flat'	10% 'steep'
$\sim 10^{17}$	25	13	+ 5	− 5
$\sim 10^{18}$	47	20	−15	+10
$\sim 10^{19}$	52	14	−30	+30

The following features should be noted:

(i) The mean core displacement is averaged over all possible core positions for a given shower size. It is about 40 m for all energies: showers falling close to the boundary of the collecting area for a particular size tend to have poorly located cores.

(ii) The size change produced by the use of incorrect distribution functions is a minimum near 10^{17} eV. This arises because $\rho(600)$ has here, for purposes of measurement, the greatest insensitivity to detailed knowledge of the lateral distribution. For 10^{19} eV the appropriate value of r is larger.

(iii) The similarity of the variation of $\rho(600)$ (table 3) to the calculated intrinsic fluctuations of similar parameters for proton primaries stresses the aptness of this quantity as the adopted parameter.

2.6. Shower flux measurements

The area within which a shower may fall and still be detected increases with shower size, and because of the steep slope of the primary energy spectrum, and of the corresponding measured $\rho(600)$ spectrum, this is a feature which has to be utilized as far as possible to improve the total rate of collection of the most energetic events. For the Haverah Park array, the area of detection with greater than 93% efficiency for vertical showers increases from 1·5 km^2 at 10^{18} eV to 11 km^2 at 10^{19} eV, and the treatment of this rapid variation is not at all straightforward.

In a method developed by the MIT group (Clark *et al* 1961) a statistical weight A^{-1} was assigned to each shower, where A was the area within which that shower could have fallen and triggered the array with greater than 93% probability. This treatment depends unduly on knowledge of the lateral distribution function at large distances, a quantity difficult to measure because of the statistical uncertainties of low intensity signals.

We have aimed to achieve a more rigorous determination of shower flux, by a method in which a 'constant area' was assigned to each 'size bin' in the following way.

Showers were binned in size intervals the limits of which were in the ratio $\sqrt{2}$ and the area for greater than 93% selection probability was calculated for the smallest shower size falling in that bin, using the empirically determined lateral distribution function. For a particular $\rho(600)$, the distance r (3·75 GeV) was determined, this being the distance at which the energy density in one of the triggering detectors falls to the selection level (§ 2.1). The 'constant area' was chosen to be 15% less than that corresponding to r (3·75 GeV) calculated for the smallest shower size in the particular bin under consideration. These areas were obtained as a function of r and θ using a numerical method.

For very large showers ($E > 10^{19}$ eV) the collecting area can be larger than the area enclosed by the (rectilinear) boundary of the whole array. However, because of the uncertainties of size determination for showers with cores falling outside the area of the array so defined, all such showers are rejected, and thus for the largest showers this sets, in effect, a limit beyond which the collecting area cannot be allowed to extend.

The method of flux measurements here differs in detail but not in principle from that given previously (Andrews *et al* 1971), and it is, of course, possible to devise other satisfactory methods of choosing a 'constant area'. Detailed computer simulations (Evans 1971) have shown, however, that if some such method is not used, then systematic distortion of the derived spectrum will occur, because, in addition to the flux being uncertain, the size measurement of rejected showers is (on average) less accurate than

for accepted ones. All such methods seem to involve some sacrifice of area over which each intensity determination can be made.

3. Experimental results

3.1. Spectra of $\rho(600)$ as a function of the zenith angle θ

The showers selected in each of the eight zenith angle bands were analysed using empirical lateral distribution functions, the derivation of which has been described in § 2.4. A $\rho(600)$ spectrum was determined for each zenith angle band by a maximum-likelihood fit to the number of showers in $\sqrt{2}$ size intervals falling in the 'constant area' assigned for each size bin. Writing the spectrum in the form:

$$I(>\rho(600)) = k(\rho(600))^{-\Gamma}, \tag{3.1}$$

the values of the parameters k and Γ are given in table 4 (k is in units 10^{-12} m^{-2} s^{-1} sr^{-1}).

Table 4.

	Zenith angle bands							
	0°–20°	20°–30°	30°–35°	35°–40°	40°–45°	45°–50°	50°–55°	55°–60°
k	5·6 ± 0·3	5·2 ± 0·3	3·5 ± 0·3	2·7 ± 0·2	2·4 ± 0·2	1·4 ± 0·1	0·94 ± 0·1	0·60 ± 0·04
Γ	1·99 ± 0·10	2·08 ± 0·09	2·11 ± 0·15	2·07 ± 0·12	2·24 ± 0·13	2·09 ± 0·11	2·25 ± 0·13	2·34 ± 0·12

3.2. Determination of attenuation length

Assuming exponential attenuation of showers in the atmosphere over the depth corresponding to the extremes of inclination, the values of $\rho(600)$ observed for showers derived from primaries of the same energy but incident at various zenith angles θ, will be related by

$$(\rho(600))_\theta \exp\left(\frac{1018}{\lambda}\sec\theta\right) = \text{constant}, \tag{3.2}$$

where λ (in g cm^{-2}) is the attenuation length (the atmospheric depth of Haverah Park being taken to be 1018 g cm^{-2}).

To derive λ, cuts at constant intensity, and so corresponding to constant primary energy, are taken across the eight spectra of the zenith angle bands. Since the experimental exponents of these spectra are not identical, the value of λ derived will depend upon the intensity at which the cut is made. At $I = 10^{-12}$ m^{-2} s^{-1} sr^{-1}, the value is 760 ± 40 g cm^{-2}. In order to determine λ also from a cut at $I = 10^{-13}$ m^{-2} s^{-1} sr^{-1} the spectral slopes were redetermined in the range $2 \times 10^{-12} > I > 5 \times 10^{-14}$ m^{-2} s^{-1} sr^{-1}, to ensure that the spectra were in correct fit to the experimental data over this particular range. The redetermined values of k and Γ differed only slightly from those initially determined (table 4), and do not support the existence of any systematic changes. The value of λ for a cut at 10^{-13} m^{-2} s^{-1} sr^{-1} is 780 ± 35 g cm^{-2}.

These values of λ and their accompanying uncertainties are determined from a least-squares fit to data: a determination of λ from a cut at still lower intensity is not practicable because of the small number of showers available. We take these results to indicate

that the spectra are consistent with exponential absorption of showers identified by the parameter $\rho(600)$ in the atmosphere, and moreover, with an attenuation length the variation of which with shower size is not detectable to the accuracy of the present work.

We have assigned to each shower a size normalized to $\theta = 13°$ (the average, zenith angle of the first zenith angle band), and the spectrum of showers with $\theta < 60°$ follows:

$$I(>\rho(600)) = (6{\cdot}1 \pm 0{\cdot}1)10^{-12}(\rho(600))^{-2{\cdot}22\pm0{\cdot}02}\ \mathrm{m}^{-2}\,\mathrm{s}^{-1}\,\mathrm{sr}^{-1}. \qquad (3.3)$$

The differential spectrum corresponding to this integral spectrum is shown in figure 5, the data for which are tabulated below (table 5).

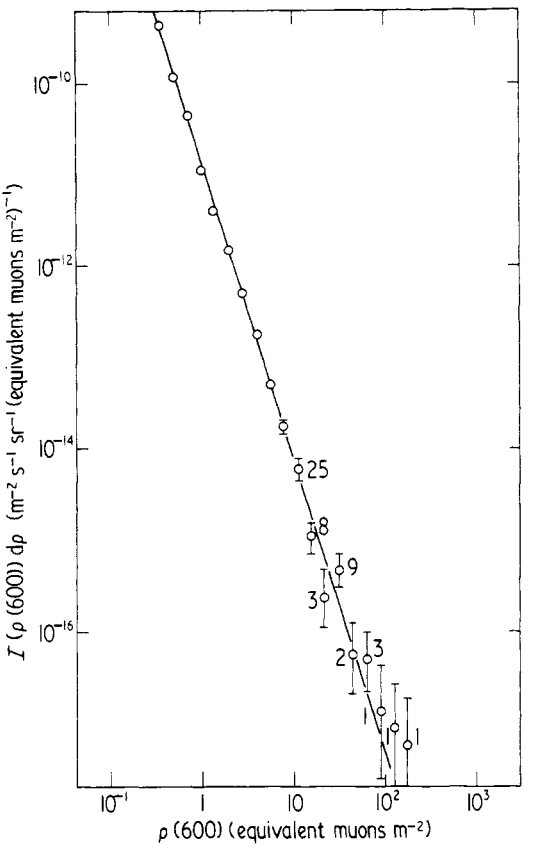

Figure 5. Differential spectrum of the ground parameter $\rho(600)$. The parameter is expressed in units of the average signal produced by a single vertical relativistic muon, and is accordingly given as equivalent muons per square metre. The differential intensity is then expressed in units $\mathrm{m}^{-2}\,\mathrm{s}^{-1}\,\mathrm{sr}^{-1}$ (equivalent muons per square metre)$^{-1}$. The figures adjacent to the points of low intensity indicate the number of showers upon which each point is based.

3.3. Spectrum distortion

It is well known that fluctuations in the measured size parameter of a shower, whether these arise from actual fluctuations of shower development or from uncertainties coming in during the process of shower sampling and the ensuing derivation of density values, can give rise to distortion of the spectrum of the measured parameter. The degree and

Table 5. Normalized differential spectrum of the parameter $\rho(600)$

Lower limit of bin $\rho(600)$ (m^{-2})	Number of showers	Intensity ($\delta\rho = 1\ m^{-2}$) ($m^{-2}\ s^{-1}\ sr^{-1}$)
0·30	350†	$4{\cdot}38 \times 10^{-10}$
0·42	200†	$1{\cdot}19 \times 10^{-10}$
0·60	155†	$4{\cdot}38 \times 10^{-11}$
0·85	162†	$1{\cdot}10 \times 10^{-11}$
1·20	511	$3{\cdot}99 \times 10^{-12}$
1·70	369	$1{\cdot}50 \times 10^{-12}$
2·40	234	$5{\cdot}13 \times 10^{-13}$
3·39	145	$1{\cdot}76 \times 10^{-13}$
4·80	72	$4{\cdot}93 \times 10^{-14}$
6·78	45	$1{\cdot}73 \times 10^{-14}$
9·60	25	$5{\cdot}72 \times 10^{-15}$
13·58	8	$1{\cdot}10 \times 10^{-15}$
19·20	3	$2{\cdot}50 \times 10^{-16}$
27·15	9	$4{\cdot}64 \times 10^{-16}$
38·40	2	$6{\cdot}49 \times 10^{-17}$
54·31	3	$6{\cdot}20 \times 10^{-17}$
76·80	1	$1{\cdot}33 \times 10^{-17}$
108·61	1	$8{\cdot}79 \times 10^{-18}$
153·60	1	$5{\cdot}77 \times 10^{-18}$

† For these bins, $\theta < 30°$, for all the remainder, $\theta < 60°$. Approximately $\rho(600) = 14$ corresponds to $E_p = 10^{19}$ eV.

manner of distortion are determined by the functional dependence of the fluctuations and uncertainties on shower size. (A comparable problem was examined by Murzin (1965) in connection with the determination of nuclear interaction parameters in emulsion.) Fluctuations and measurement uncertainties can be formally treated in the same way, because, for a fixed 'input' energy or size, the 'output' is approximately log-normally distributed, the width of this distribution being characterized by σ, the log-normal standard deviation. If σ is independent of primary energy or shower size, then a spectrum which was initially described by a single constant index will be unchanged in slope except close to the threshold of detection, while the intensity will be overestimated at each shower size. This overestimation of intensity is not large, being only about 2% for measurement uncertainties of 20% ($\sigma = 0{\cdot}08$).

However, in real experiments on large showers, the resolution is almost always not constant, and it tends to deteriorate with increasing primary energy. The best estimates for the selected material from Haverah Park used in the present work are that the resolution decreases from about 13% to values which might be as large as 30% between 3×10^{17}eV and 10^{19} eV. A change of resolution in this sense will give rise, from a true spectrum of constant index, to an observed one in which the spectrum at the lower energies correctly describes the true spectrum but for which at higher energies a flattening of the spectrum may become evident. This feature is of importance both for the general interpretation of any apparent flattening of size parameter spectrum which is encountered in experimental work and also for the effect which it may have upon the way in which a rapid change of the true spectrum (eg the Greisen effect) would be exhibited in the experimentally determined spectrum.

We have investigated the problems of these distortions using a two-stage Monte Carlo technique. From an adopted primary spectrum, a sample of 'N' showers is

randomly selected and the 'measured' size of each shower is found by sampling randomly from the log-normal 'output' distribution characteristic of the 'input' size. A resultant measured spectrum is thus assembled. This procedure was carried out for a statistical sample at Haverah Park corresponding to the present work ($N \sim 3500$) and with the resolution values estimated in the previous paragraph. Assuming a real incident spectral index of -2 (integral), the derived spectrum is indistinguishable (within better than 5%) from the initial value. Accordingly, if our estimates of resolution are correct, (and we hope that the deterioration is in fact an overestimate), we expect our measured spectrum to represent correctly that of showers falling upon it in the range 3×10^{17} to 10^{19} eV.

However the material to which these conclusions relate forms a very rigorously selected sample, and there can be no doubt that in some earlier work much less favourable conditions of resolution at high energies are to be encountered. As an example of the effect of the inclusion of seriously uncertain material, we show in figure 6(*a*) the effect of simulating a reduction of resolution from 13% to 200% over a range of energy of two decades: σ was assumed to vary as $\sigma = 0{\cdot}05 + 0{\cdot}2 \lg E/E_0$. This example although intended to be extreme, is not in our view far beyond what has been used in the past. It shows strong flattening of the spectrum which comes into effect at little more than ten times the threshold energy beyond which deterioration of resolution of the form indicated was assumed, the spectral index being reduced from the initial value of -2, which is correctly reproduced at the lower energies, to about $-1{\cdot}3$ over the later section.

Finally, we have carried out a simulation to exhibit the way in which changes of resolution would effect the possibility of detection of a Greisen-type cut-off. In figure 6(*b*) a primary spectrum of constant index but subject to a complete cut-off at $16E_0$ ($E_p \sim 3 \times 10^{19}$ eV) was introduced and the anticipated measured spectrum derived: (*a*) using the large uncertainties arising from the variation of σ used in the last example; and (*b*) using the change of resolution which we think represents the sample now being

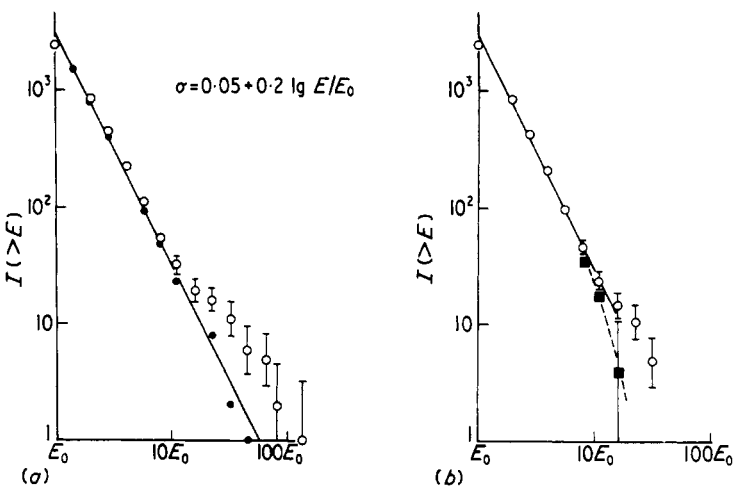

Figure 6. Features of spectrum distortion illustrated from a group of about 3000 simulated showers. In (*a*), from the assumed spectrum (full line) the actual spectrum of a 3000 shower sample is shown as full circles. The open circles show the spectrum derived when measurement uncertainties increase rather rapidly with primary energy. In (*b*), the input spectrum is assumed sharply cut-off at $16E_0$. The open circles show the deduced spectrum under the same conditions of resolution as for the corresponding points in (*a*); the full squares show the spectrum deduced for the resolution presently operative at Haverah Park.

derived from Haverah Park. The conclusion is that the extreme variation of resolution would entirely obscure the cut-off, but in a sample of the size now under examination, and with the resolution we think applicable to the present Haverah Park material, it would be detectable, although with some distortion.

We consider the particular problems of distortion at the highest studied energies in § 4.4.

4. Discussion

4.1. Models and their use

Ground-based observations and the ultimate objective of study, for the present paper the spectrum of total energy of incident primaries, are linked by model predictions of the intervening shower development and in particular of the nuclear physics which most strongly controls it. Such models must relate reasonably with well established data at machine energies but, since we are using an extrapolation of six orders of magnitude, this is a very mild constraint. The retention or rejection of models seriously postulated must accordingly rest essentially on the degree of internal consistency of their predictions with the whole range of shower observations of whatever sort.

In what follows, frequent reference is made to the series of model predictions made by A M Hillas and his co-workers (Hillas 1970, Hillas *et al* 1971a, b) and the nomenclature used is that which they established. The use of this group of models is based on the view that they represent a reliable and well chosen group, and particularly because they have been examined with direct reference to the $\rho(r)$ parameter which is that upon which the Haverah Park spectrum studies are based. This concentration upon a single group of models does not of course imply that no others are important for shower studies at these energies, but we regard it as essential to concentrate upon models which can be related confidently to the actual nature of our own measurements.

4.2. Comparison with other measurements of the spectrum

In figure 7 we compare the data on the spectrum of $\rho(600)$ derived in this paper with that reported in the work of Bell *et al* (1971) for the spectrum of the total number of muons in showers detected with the large Sydney air shower array.

This work in fact gives spectra for four zenith angle ranges, each of which corresponds to a different muon energy threshold: our comparison is with the best determined group, centred on the vertical and with $\theta < 33°$; this group corresponds to a muon energy threshold of about 0·82 GeV.

The spectra of $\rho(600)$ and of N_μ will be seen to be of very closely the same spectral index, within about 1 %, but this extreme similarity must be regarded as fortuitous, since neither experiment can be yielding information which, including systematic shortcomings, is certain to this accuracy.

Hillas *et al* (1971a, b) give the relationship between N_μ and E_p for eight different models in the form:

$$N_\mu \sim E_{\mathrm{p}}^{\beta}, \tag{4.1}$$

and in table 6 these values of β† are given together with those of α, the corresponding

† Hillas and his co-workers, in the papers referred to, give values of β for about 0·32 GeV and about 10 GeV: we quote the former of these sets.

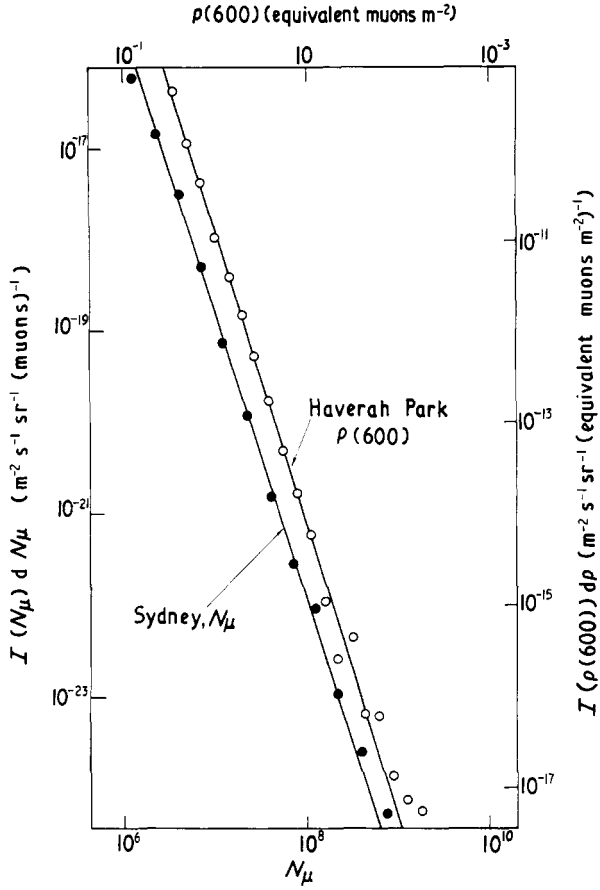

Figure 7. Comparison of the spectra of the ground parameter $\rho(600)$, measured at Haverah Park, and N_μ measured at the University of Sydney array.

index in the relation:

$$\rho(600) \sim E_p^{\alpha}, \tag{4.2}$$

for primary masses, $A = 1$, 10 and 50. The values for 10 and 50 come from a simple approximation which does not include details of fragmentation mechanisms, but the general tendency of refinements in this respect are more likely to bring the value of α for heavy primaries nearer to those for $A = 1$ than to make them more different. The tabulated values of α stress the features of the parameter $\rho(600)$ to which we attach particular importance: its insensitivity to changes of model and of primary mass.

In the final column of table 6, the quantity $\bar{\alpha} - \beta$ is indicated: it is relevant because on present information the measured value of this quantity appears to be very small, probably about 0·01, although it is not possible to give a useful estimate of the precision of this near identity of spectral form.

Since the spectra of $\rho(600)$ and N_μ are similar, a constant of equivalence, representing the ratio between these two parameters (each in appropriate units) can readily be derived which is not strongly energy sensitive. This feature is examined in § 4.3 below.

Table 6.

Model	α, $A = 1$	α, $A = 10$	α, $A = 50$	β	$\bar{\alpha} - \beta$
A	0·98	0·97	0·97	0·94	0·03
D	0·99	1·00	0·99	0·91	0·08
E	0·98	0·98	0·98	0·94	0·04
F	0·98	0·97	0·97	0·95	0·02
H	0·99	0·99	0·99	0·97	0·02
I	0·97	0·97	0·97	0·92	0·05
J	0·98	0·98	0·98	0·96	0·02
K	0·98	0·98	0·99	0·92	0·06

In figure 8, we compare the well known data of Linsley (1963a) with recent results reported from the Yakutsk, MSU, Lebedev Institute collaboration at Yakutsk, given by Diminstein *et al* (1972). Both of these experiments relate to determination of the quantity N_e, and already we have indicated some difficulties in using this as a shower parameter; we have not the information to determine whether these two experiments yield measurements of strictly comparable nature. However, what is striking is the similarity of the results when plotted together. Moreover, the feature which attracted so much attention when Linsley's results were first published (and which tended to be more strongly stressed by others than by the author himself), that there was a region from about 10^{18} eV upwards over which the spectrum showed a diminished index (the so called 'ankle') seems much less important when these two sets of data are seen together. What now seems a more

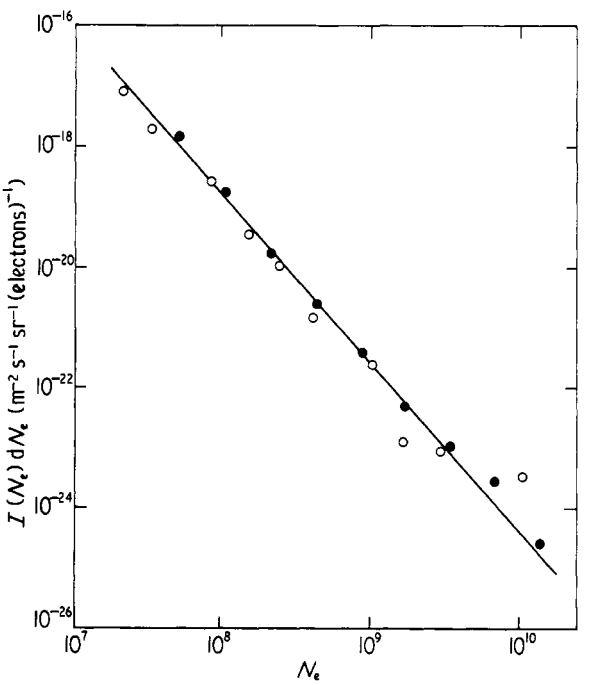

Figure 8. The spectrum of N_e (number of electrons) as shown in work at Volcano Ranch (full circles, Linsley 1963a) and at Yakutsk (open circles, Diminstein *et al* 1972).

informative approach is to regard the total data as defining a single-index N_e spectrum. Thus:

$$\Gamma(N_e) \sim 2{\cdot}8 \text{ (differential)}, \tag{4.3}$$

and accordingly the evidence is that $\Gamma(N_e)$ is significantly different from $\Gamma(N_\mu)$ and $\Gamma(\rho(600))$, which are closely similar.

We do not think that the information we now have allows a close evaluation of this difference to be undertaken. An essential difference between the $\rho(600)$ spectrum and the N_μ spectrum on the one hand and the two N_e spectra on the other is that the former pair are analysed using a lateral distribution function which does not vary with energy, while the latter both make use of a similarly defined energy-sensitive distribution function. The justification of either procedure is complex, and not to be attempted except with full access to the primary data of the particular piece of work. At an earlier stage of the Haverah Park work (Andrews *et al* 1970) a distribution function varying with energy was thought to have been established and was used, but after very detailed and rigorous work, we conclude that any variation which may exist is much smaller than we had previously supposed.

4.3. Status of Hillas models

We have already shown that the slopes of the $\rho(600)$ spectrum which is the subject of the present work and the N_μ spectrum reported by Bell *et al* (1971) are indistinguishable: accordingly a measured ratio of these two quantities is readily derived:

$$N_\mu/\rho(600) = 3{\cdot}9 \times 10^6 \text{ muons/equivalent muon m}^{-2}.$$

In table 7 this measured ratio is compared with the values predicted by the Hillas models. The quoted figures are all for $A = 1$, and predictions are energy sensitive. The first approximation values for other values of A are given by treating the resultant shower from $A = n$ as the superposition of n showers each of primary energy E_p/n: here for example, the values for $E_p = 10^{18}$ eV and for $A = 10$ would be those tabulated under $E_p = 10^{17}$ eV. However, the tendency of detailed fragmentation models will be to yield something between a proton shower and that predicted in this most simple way, and so the values appropriate for $A = 10$ are probably rather smaller than those derived by it. The region of maximum measurement accuracy for the ratio of the results of these two entirely distinct experiments is, of course, not known, but it must certainly lie nearer to

Table 7. Model predictions of $(N_\mu/\rho(600))10^{-6}$ as a function of primary energy

	Primary energy (eV)		
Model ($A = 1$)	10^{17}	10^{18}	10^{19}
A	5·0	4·4	4·2
D	3·6	2·9	2·4
E	4·6	4·3	3·9
F	4·9	4·6	4·3
H	5·6	5·1	4·8
I	4·2	3·8	3·4
J	4·9	4·5	4·3
K	3·7	3·1	2·7

10^{18} eV than to either 10^{17} eV or 10^{19} eV, and probably rather greater than 10^{18} eV. We therefore argue on the basis that it is $E = 10^{18}$ eV+.

Taking account of the data in tables 6 and 7, together with the independent muon measurements of Blake *et al* (1971) at Haverah Park, which refer to rather lower muon energies and to observations over distances 150 m–500 m from the shower axis, only model D seems on all accounts unsatisfactory. Beyond this, the present analysis reinforces the conclusion reached by Blake and his co-workers that E and I are most strongly indicated; K appears less suitable, and indeed is not one of the better models unless the primary mass is high. Model H, as well as D, seems inadequate.

Thus the models supported here require $n_s \sim E_{rad}^{1/4}$ at all energies, and are altogether consistent with isobar production.

4.4. The spectrum of $\rho(600)$ at extreme energies ($>10^{19}$ eV)

The spectrum shown in figure 5 can be defined confidently up to nominal energies of about 10^{19} eV by the differential power index $(-3{\cdot}22 \pm 0{\cdot}02)$. At higher energies there are few showers, less than thirty, and here the evidence can only be as to whether these provide serious indication of any departure from this power law. We conclude that they do not: any evidence of this character would have to be related to the points on the graph coming from the six showers of greatest energy out of a total of more than 3000!

The extent to which these showers lead to points lying above the line determined at lower energies could in the first place readily occur as a matter of statistical fluctuation; also detailed examination shows that the form of distortion indicated in § 3.3 cannot be completely excluded in this group. Finally the most energetic shower included, which corresponds to a primary energy rather above 10^{20} eV, provides an interesting example of the problem encountered at the extreme end of a spectrum such as studied here. The core of this particular shower is computed to fall about 30 m within the perimeter of the assigned collecting area: it is not a specially well determined core position and the asymmetry of the possible area into which it might have fallen makes it realistic to regard it as having an almost 50/50 chance of having in fact fallen inside or outside the collecting area. (The actual $\rho(600)$ measurement is relatively good.) Had this been one of many comparable showers, the procedure which has already been outlined would have led, on average, to as many such events moving into the collecting area as out, but this in not the position: of the most energetic showers, this is the only one for which the core location is so close to the boundary of the collecting area!

We thus conclude that there is no evidence, up to the highest measured energies, of any variation of the slope of the differential $\rho(600)$ spectrum. This slope is well determined up to primary energies of about 10^{19} eV, and consistent with all higher energies.

4.5. The primary energy spectrum

Equation (3.3) gives the adopted form of the $\rho(600)$ spectrum normalized for near-vertical incidence, and we have indicated in the previous paragraph that this fits the data at all energies above about 3×10^{17} eV. We now consider the conclusion that follows about the primary total energy spectrum, using the relationship (4.2) for the various models considered. If we write the spectrum in the form:

$$I(>E_p) = k10^{-10}\left(\frac{E_p}{10^{17}}\right)^{-\gamma} \text{m}^{-2}\,\text{s}^{-1}\,\text{sr}^{-1} \tag{4.4}$$

the derived value of the k and γ for the six models retained at the end of § 4.3 are given in table 8.

Table 8 brings out very strongly the extent which the parameter $\rho(600)$ is only slightly sensitive both to the mass of the incident primary and over a range of very different models of shower development, and therefore its fitness to lead to a statement of the

Table 8. Spectrum constants for various models and primary masses

	$A = 1$		$A = 10$		$A = 50$	
Model	k	γ	k	γ	k	γ
A	3·1	2·16	2·6	2·16	2·4	2·15
E	4·3	2·18	3·9	2·17	3·6	2·17
F	2·0	2·17	1·8	2·16	1·6	2·15
I	4·5	2·15	3·9	2·15	3·5	2·15
J	3·6	2·18	3·3	2·18	3·1	2·18
K	—	—	6·0	2·18	5·8	2·19

total energy spectrum of primary particles†. As examples only, we quote here the spectra for the three most favoured Hillas models, E and I for $A = 1$ and $A = 10$; K for $A = 50$:

model E ($A = 1$)

$$I(>E_p) = (4{\cdot}3 \pm 0{\cdot}1)10^{-10}\left(\frac{E_p}{10^{17}}\right)^{-2{\cdot}18\pm0{\cdot}02} \text{ m}^{-2}\,\text{s}^{-1}\,\text{sr}^{-1}, \tag{4.5}$$

model E ($A = 10$)

$$I(>E_p) = (3{\cdot}9 \pm 0{\cdot}1)10^{-10}\left(\frac{E_p}{10^{17}}\right)^{-2{\cdot}17\pm0{\cdot}02} \text{ m}^{-2}\,\text{s}^{-1}\,\text{sr}^{-1}, \tag{4.6}$$

model I ($A = 1$)

$$I(>E_p) = (4{\cdot}5 \pm 0{\cdot}1)10^{-10}\left(\frac{E_p}{10^{17}}\right)^{-2{\cdot}15\pm0{\cdot}02} \text{ m}^{-2}\,\text{s}^{-1}\,\text{sr}^{-1}, \tag{4.7}$$

model I ($A = 10$)

$$I(>E_p) = (3{\cdot}9 \pm 0{\cdot}1)10^{-10}\left(\frac{E_p}{10^{17}}\right)^{-2{\cdot}15\pm0{\cdot}02} \text{ m}^{-2}\,\text{s}^{-1}\,\text{sr}^{-1}, \tag{4.8}$$

model K ($A = 50$)

$$I(>E_p) = (5{\cdot}8 \pm 0{\cdot}1)10^{-10}\left(\frac{E_p}{10^{17}}\right)^{-2{\cdot}19\pm0{\cdot}02} \text{ m}^{-2}\,\text{s}^{-1}\,\text{sr}^{-1} \tag{4.9}$$

where, in every instance, E_p is measured in eV.

The principal conclusion, therefore, of this work is that, in spite of the uncertainty of knowledge both of the composition of primary particles and of the details of shower

† Dr K E Turver (private communication) has given us information about the anticipated relationship between $\rho(600)$ and primary energy at $E = 10^{17}$ eV for a variety of other models. All reinforce the point made in the text as to the model insensitivity of this ground parameter.

development, a confident description of the total energy spectrum of primaries can be given in the form:

$$I(>E_p) = (4{\cdot}5 \pm 0{\cdot}5)10^{-10}\left(\frac{E_p}{10^{17}}\right)^{-2{\cdot}17\pm0{\cdot}03} \text{ m}^{-2}\,\text{s}^{-1}\,\text{sr}^{-1}, \tag{4.10}$$

well determined over the energy range 3×10^{17} eV–10^{19} eV, and with all observations beyond 10^{19} eV entirely consistent with the continuation of this form of spectrum up to 10^{20} eV. This indicates a rate of arrival of primaries with $E_p > 10^{20}$ eV of the order of $0{\cdot}03\,\text{km}^{-2}\,\text{a}^{-1}$.

Comparing equation (4.10) with the earlier work of Andrews *et al* (1971), the greater uncertainty of the intensity now quoted is entirely a statement of the range possible under the models which remain plausible. The change of index is not mainly linked with variations of model, but rather reflects the effect of more experienced shower analysis and the use of a more soundly established lateral distribution function.

4.6. Relationship of the primary spectrum (present range) with that at lower energies

Over recent years only a limited amount of work has been reported on the region of primary spectrum, 10^{15} eV–3×10^{17} eV, which falls immediately below that of the present work. It is a region where the interpretation of sea-level work is not easy, but data are available from observations at Chacaltaya, where measurements are possible near to shower maximum. La Pointe *et al* (1968) working at Chacaltaya give the spectrum over this range in the form:

$$I(>E_p) = (2{\cdot}0 \pm 0{\cdot}4)10^{-10}\left(\frac{E_p}{10^{17}}\right)^{-2{\cdot}2\pm0{\cdot}15} \text{ m}^{-2}\,\text{s}^{-1}\,\text{sr}^{-1}, \tag{4.11}$$

which we may compare with the value given in equation (4.10) above. This spectrum is close to that earlier reported from Chacaltaya by Bradt *et al* (1965), and while this is not explicitly stated, probably follows Toyoda *et al* (1965) in regarding the primary particles as protons.

The spectra (equations (4.10), (4.11)) cannot be uniquely related, since they are the products of such different modes and conditions of observation and analysis. If, for example, the Haverah Park data were interpreted by use of model F (table 8) for $A = 1$, the spectra would be identical! Since in both experiments, however, and in others like them, the index is derived with much more confidence than the absolute intensity we would minimize the importance of the latter, although noting that model K is that which leaves the largest fitting problem. We suggest that the combined results above all provide evidence of no significant difference of index over the whole range from 10^{15} eV to 10^{20} eV.

5. Summary and conclusions

(i) The primary total energy spectrum has the form:

$$I(>E_p) = (4{\cdot}5 \pm 0{\cdot}5)10^{-10}\left(\frac{E_p}{10^{17}}\right)^{-2{\cdot}17\pm0{\cdot}03} \text{ m}^{-2}\,\text{s}^{-1}\,\text{sr}^{-1}$$

over the energy range 3×10^{17} eV–10^{19} eV, and there is no evidence of any deviation from this form up to 10^{20} eV.

(ii) The present work can best be related to that at Chacaltaya (La Pointe *et al* 1968) by assuming that the above expression holds also over the range

$$10^{15} \text{ eV} < E_p < 3 \times 10^{17} \text{ eV}.$$

(iii) Since the whole mode of treatment is directed to minimizing the sensitivity of the measurement to model assumptions in shower development, discrimination among models is not strong. What indications there are, and the confidence to be placed in them, are developed in the main text.

(iv) The lack of structure in the spectrum over the whole range 10^{15}–10^{20} eV is relevant to galactic containment and to interaction with residual microwave radiation.

There is no indication in this range of any feature which might be related to a cross-over from a predominantly galactic to a predominantly extragalactic origin of the primary particles. Work in the Haverah Park group (Lapikens *et al* 1971) has established that the flux is highly isotropic at, and somewhat above, 10^{17} eV. Reviewing evidence in 1971, Stecker (1971) came to the conclusion that the features then beginning to become apparent, and particularly the absence of any 'ankle' effect, were best described in terms of the galactic origin and containment of all cosmic ray particles, accepting the implication that those of the highest energy must be heavy.

The general facts upon which his conclusion was based are strengthened in our present work. However, a single feature is strongly and probably decisively against it. One of the largest showers, for which the estimate of primary energy is $1{\cdot}3 \times 10^{20}$ eV, is observed to come from the direction $\alpha = 199°$, $\delta = 44°$, close to that of the N galactic pole ($\alpha = 187°$, $\delta = 27°$). Following Ginzburg and Syrovatskii (1971), and using a value of magnetic field $0{\cdot}4\gamma$ over a distance of 1000 pc (3×10^{19} m), the total deflection of an *iron nucleus* entering through this field (with the field always in a direction to lead to maximum final deflection) would be about 45°. Since the optimization of field direction used here can hardly be realistic, a significantly smaller deflection must in all likelihood be implied, and we would regard this primary as certainly metagalactic. There is, of course, no evidence that it is indeed an iron nucleus.

(v) As to interaction with residual microwave photons, nothing in our observation supports the various proposals for features which might be expected to be detectable at energies significantly below 10^{20} eV. However, Stecker (1968), using a revised value of the photo-meson cross section and the rather lower temperature (2·7 K) of the residual radiation now accepted, has indicated that no significant attenuation of (proton) primaries of 10^{20} eV will take place over distances of about 300 Mpc. Further, Stecker has shown that protons of all energies (up to 10^{22} eV) can reach us without attenuation from distances of about 10 Mpc, the dimension of the local super-cluster of galaxies. However, if the intergalactic field is not greater than $10^{-3}\gamma$, such higher energy particles may retain directional evidence of their source.

6. Acknowledgments

This work was made possible by the establishment by the Science Research Council of the facilities at the Haverah Park Research Station, and the authors wish to record their appreciation of the opportunity to work there and their indebtedness to the Council for the support given over the period during which this work has been undertaken.

One of us (DME) thanks the University of Leeds for the award of a Junior Ellison Fellowship, and another (HJG) the Science Research Council for the award of a studentship.

References

Andrews D, Evans A C, Reid R J O, Tennent R M, Watson A A and Wilson J G 1970 *Acta Phys. Acad. Sci. Hung.* **29** *Suppl.* 3 348–8

Andrews D *et al* 1971 *Proc. 12th Int. Conf. on Cosmic Rays, Hobart* vol 3 (Hobart: University of Tasmania) pp 995–1000

Bell C J *et al* 1971 *Proc. 12th Int. Conf. on Cosmic Rays, Hobart* vol 3 (Hobart: University of Tasmania) pp 989–93

Blake P R, Ferguson H, Nash W F and Thomas D W E 1971 *Proc. 12th Int. Conf. on Cosmic Rays, Hobart* vol 3 (Hobart: University of Tasmania) pp 1044–49

Bradt *et al* 1965 *Proc. 9th Int. Conf. on Cosmic Rays, London* vol 2 (London: The Institute of Physics and The Physical Society) pp 715–7

Clark G W *et al* 1961 *Phys. Rev.* **122** 637–54

Diminstein O C *et al* 1972 *Rep. at 3rd European Symp. on High Energy Interactions and Extensive Air Showers, Paris* unpublished

Evans A C 1971 *PhD Thesis* University of Leeds

Ginzburg V L and Syrovatskii S I 1971 *Proc. 12th Int. Conf. on Cosmic Rays, Hobart* (Hobart: University of Tasmania) Invited and Rapporteur Papers pp 53–71

Greisen K 1966 *Phys. Rev. Lett.* **16** 748–50

Hillas A M 1968 *Can. J. Phys.* **46** S623–6

—— 1970 *Acta Phys. Acad. Sci. Hung.* **29** *Suppl.* 3 355–60

Hillas A M, Marsden D J, Hollows J D and Hunter H W 1971a *Proc. 12th Int. Conf. on Cosmic Rays, Hobart* vol 3 (Hobart: University of Tasmania) pp 1001–6

Hillas A M, Hollows J D, Hunter H W and Marsden D J 1971b *Proc. 12th Int. Conf. on Cosmic Rays, Hobart* vol 3 (Hobart: University of Tasmania) pp 1007–12

Kawaguchi S *et al* 1971 *Proc. 12th Int. Conf. on Cosmic Rays, Hobart* vol 7 (Hobart: University of Tasmania) pp 2736–41

Kraushaar W L 1958 *Suppl. Nuovo Cim.* **2** 649–52

Lapikens J *et al* 1971 *Proc. 12th Int. Conf. on Cosmic Rays, Hobart* vol 1 (Hobart: University of Tasmania) pp 316–20

La Pointe M *et al* 1968 *Can. J. Phys.* **46** S68–71

Linsley J 1963a *Proc. 8th Int. Conf. on Cosmic Rays, Jaipur* vol 4 (Bombay: TIFR) pp 77–99

—— 1963b *Proc. 8th Int. Conf. on Cosmic Rays, Jaipur* vol 4 (Bombay: TIFR) pp 295–305

Murzin V S 1965 *Proc. 9th Int. Conf. on Cosmic Rays, London* vol 2 (London: The Institute of Physics and The Physical Society) pp 872–4

Stecker F W 1968 *Phys. Rev. Lett.* **21** 1016–8

—— 1971 *Nat. Phys. Sci.* **234** 28–9

Tennent R M 1967 *Proc. Phys. Soc.* **92** 622–31

Toyoda Y *et al* 1965 *Proc. 9th Conf. on Cosmic Rays, London* vol 2 (London: The Institute of Physics and The Physical Society) pp 708–11

Williams R W 1948 *Phys. Rev.* **74** 1689–706

Zatespin G T and Kuzmin V A 1966 Soc. Phys.–*JETP* **4** 114–7